JOURNAL OF AGRICULTURAL AND FOOD CHEMISTRY

Aggregation of β-Lactoglobulin Regulated by Glucosylation

KERENSA BROERSEN,*,†,§ MARIJKE ELSHOF,§ JOLAN DE GROOT,§ ALPHONS G. J. VORAGEN,§ ROB J. HAMER,†,§ AND HARMEN H. J. DE JONGH†,#

Wageningen Centre for Food Sciences, Diedenweg 20, P.O. Box 557, 6700 AN Wageningen, The Netherlands; Laboratory for Food Chemistry, Wageningen University and Research Centre, Bomenweg 2, 6700 EV Wageningen, The Netherlands; and TNO Quality of Life, Utrechtseweg 48, 3704 HE Zeist, The Netherlands

A large number of proteins are glycosylated, either in vivo or as a result of industrial processing. Even though the effect of glycosylation on the aggregation of proteins has been studied extensively in the past, some reports show that the aggregation process is accelerated, whereas others found that the process is inhibited by glycosylation. This paper investigates the reasons behind these controversial results as well as the potential mechanism of the effect of glucosylation on aggregation using bovine β-lactoglobulin as a model. Glucosylation was found to inhibit denaturant-induced aggregation, whereas heat-induced aggregation was accelerated. It was also found that the kinetic partitioning from an unfolded state was driven toward refolding for glucosylated protein, whereas aggregation was the preferred route for the nonglucosylated protein.

KEYWORDS: Aggregation; glucosylation; β-lactoglobulin; hydrophobicity; electrostatic repulsion; unfolding/refolding

INTRODUCTION

Glycosylation as a result of industrial processing significantly affects the aggregation properties of proteins (*1*, *2*). Conjugation of chitosan to β-lactoglobulin (βlg) by the Maillard reaction, a reaction brought about by a number of food-processing conditions, has been found to suppress protein aggregation (*3*). Also, the in vivo glycosylation of proteins affects the aggregation reaction (*4*, *5*). For example, human erythropoietin was shown to be more susceptible to aggregation upon the removal of N-linked oligosaccharides (*5*). Glycan chains attached to nascent proteins are believed to promote correct folding, preventing protein aggregation (*6*−*8*). Conversely, posttranslational glycosylation of lens proteins has been shown to induce conformational changes and unfolding of proteins resulting in aggregation (*9*). These examples demonstrate that carbohydrate chains play an essential role in regulating the aggregation process of proteins in general. The mechanism by which glycosylation intervenes with the aggregation reaction of proteins is not currently known and is the subject of this paper.

Several studies suggested for a wide range of proteins that glycosylation affects the hydrophobicity, net charge, and heat stability—each determinants of the aggregation process (*10*−*13*). Other studies confirmed that the folding rate of proteins can be enhanced by the covalent attachment of sugar moieties (*11*, *14*). The aggregation-regulating effect of glycosylation has thus been directly related to the kinetic partitioning between folding and aggregation, and this may provide a potential explanation. An alternative hypothesis can be derived from the attractive association of proteins to form aggregates, which are often driven by hydrophobic interactions; aggregation could be inhibited by the reduced hydrophobicity as a result of the glycosylation. Also, electrostatics can be affected by glycosylation: the attachment of sugar moieties to the protein by the Maillard reaction reduces the number of positive charges and produces a protein with a different net charge. This change in net charge affects electrostatic repulsion, potentially resulting in an altered tendency of proteins to aggregate. In view of the wide occurrence of glycosylation reactions (*11*), the recently established relationship between protein aggregation and a number of detrimental diseases (*15*, *16*), and its application in biotechnological and food systems (*17*, *18*), the elucidation of the mechanism of aggregation inhibition through glycosylation provides the means to understand protein aggregation reactions in all of these areas.

In this work, monosaccharides were conjugated to the surface of bovine β-lactoglobulin to investigate the effect of glucosylation on the aggregation properties of proteins. The thermodynamic consequences of the procedure employed have been recently investigated for β-lactoglobulin (*13*). In this paper we will report our findings on the investigation of the aggregation propensity, providing further insight into the action of glycosylation on the aggregation of proteins. We will apply heat- and urea-induced aggregation conditions and we will report on

* Address correspondence to this author at the MRC Laboratory of Molecular Biology, Neurobiology Division, Hills Road, Cambridge CB2 2QH, United Kingdom [telephone +44 (0)1223 402316; fax +44 (0)1223 402310; e-mail broersen@mrc-lmb.cam.ac.uk].
† Wageningen Centre for Food Sciences.
§ Wageningen University and Research Centre.
# TNO Quality fo Life.

10.1021/jf063178z CCC: $37.00
Published on Web 02/28/2007

the potential involvement of electrostatics and hydrophobicity on aggregation kinetics upon glucosylation.

MATERIALS AND METHODS

Protein Purification and Modification. *Isolation and Purification.* Bovine βlg was isolated and purified (>98% purity) from fresh cow's milk (A:B ratio 60:40) using a protocol described previously (*19*).

Preparation of Glucosylated Proteins. Typically, 0.27 mM protein was dissolved in demineralized water. Per milliliter of protein solution, 28 mM D-glucose (Sigma) was added. The pH was adjusted to 8.0 using 1 M NaOH, and the mixture was lyophilized. Next, the mixture was incubated at 60 °C for 5 h at a relative humidity of 65% (atmosphere equilibrated with supersaturated $NaNO_2$ solution). The incubated samples were next dissolved in demineralized water and dialyzed against demineralized water to remove all of the nonreacted sugar from the solution. See also ref (*13* for details of this procedure. Subsequently, the solutions were lyophilized and stored at −20 °C until use. Throughout the paper, nonglucosylated βlg will be referred to as "βlg" and the glucosylated fraction as "Gβlg".

Protein Characterization. *Matrix-Assisted Laser Desorption/Adsorption Ionization Time-of-Flight Spectroscopy (MALDI-TOF MS).* MALDI-TOF mass spectra were acquired to determine the degree of modification as reported previously (*13*) on a Voyager-DE RP (PerSeptive Biosystems Inc.) using a 3,5-dimethoxy-4-hydroxycinnamic acid matrix.

Chromogenic o-Phthaldialdehyde (OPA) Assay. The degree of modification of the primary amino groups was determined indirectly on the basis of the specific reaction between OPA and free primary amino groups in proteins by a chromogenic assay described previously (*20*). All measurements were performed in duplicate and corrected for protein-free sample. The protein concentration was determined by the adsorption at 280 nm using an extinction coefficient of 0.659 M^{-1} cm^{-1}.

Structural Analysis. *Circular Dichroism (CD) Spectroscopy*. CD spectra of 5.5 μM (far-UV) and 0.55 μM (near-UV) βlg and Gβlg in a 10 mM sodium phosphate buffer (pH 7.0) were recorded using a Jasco J-715 spectropolarimeter (Jasco Corp.) at 25 °C in the spectral range from 260 to 190 nm (far-UV CD) or 250−350 nm (near-UV CD) with a spectral resolution of 0.5 nm. Spectra were recorded as averages of 16 scans. The scanning speed was 100 nm/min, and the response time was 0.50 s with a bandwidth of 1.0 nm. Quartz cuvettes with optical paths of 1 mm (far-UV CD) and 10 mm (near-UV CD) were used. The spectra were corrected for the corresponding protein-free sample.

Fluorescence Spectroscopy. Emission fluorescence spectra of βlg and Gβlg at a concentration of 2.7 μM in a phosphate buffer (10 mM, pH 7.0) were obtained using a Cary Med Eclipse (Varian) fluorometer at 25 °C. The emission spectra from 300 to 400 nm were determined using an excitation wavelength of 295 nm. Excitation and emission slit widths were 5 nm, and a scan speed of 100 nm/min was used. All spectra were recorded in duplicate and corrected for the corresponding protein-free sample.

Isoelectric Focusing (IEF). The apparent isoelectric points of the βlg and Gβlg were determined using the Phast System (Pharmacia). Four microliters of 1.0 mg/mL protein solutions was applied to IEF gels with a pH gradient ranging from 2.5 to 6.5 (Pharmacia) and from 3 to 10 (Pharmacia). The gels were fixed with 20% trichloric acid, stained using Coomassie Brilliant blue (R-250), and destained in 30% methanol/10% acetic acid.

Electrophoretic Titration (ETC). Nonglucosylated βlg and Gβlg were dissolved at a protein concentration of 55 μM in demineralized water. A pH gradient was generated on a ready-to-use IEF gel (3−9, Amersham) on a PhastSystem using 2000 V, 2.0 mA, 3.5 W, and 75 Vh at 15 °C. After the gel had been rotated 90° for the second dimension, the samples were applied to the gel, and the gel separated the fractions at 200 V, 2.0 mA, and 3.5 W for 15 Vh at 15 °C. The gels were fixed with 20% trichloric acid, washed with destaining solution (30% methanol, 10% acetic acid v/v), stained with 0.02% Coomassie Brilliant blue R 350 [10%; 0.2% Coomassie Brilliant blue R350 (Pharmacia) in 90% destaining solution], and subsequently destained with destaining solution.

Sodium Dodecyl Sulfate−Polyacrylamide Gel Electrophoresis (SDS-PAGE). SDS-PAGE was performed using a previously described protocol (*21*). A 15% (w/v) acrylamide separating gel and a 4% (w/v) acrylamide stacking gel containing 0.1% SDS (w/v) were run using a Mini-Protean II electrophoresis cell (Bio-Rad). Samples of 0.1 mM protein were prepared in sample buffer containing 10% SDS (w/v) and 1.25% β-mercaptoethanol (w/v). Gels were stained with Coomassie Brilliant blue R-250 and destained with 30% methanol/10% acetic acid in water (v/v).

Dynamic Light Scattering. Dynamic light scattering measurements were performed using an ALV-5000 multibit multi-tau correlator and a Spectra Physics solid-state laser operating with vertically polarized light with a wavelength of 532 nm. The range of scattering wave vectors covered $3.0 \times 10^{-3} < q < 3.5 \times 10^{-2}$ mm^{-1} [$q = 4\pi n_s \sin(\theta/2)\lambda$, where θ is the angle of observation and n_s is the refractive index of the solution]. The temperature was controlled by a thermostat bath at 25 ± 0.1 °C.

Hydrophobic Interaction Chromatography (HIC). Nonglucosylated βlg and Gβlg were dissolved at a concentration of 0.16 mM in 1 M ammonium sulfate and 10 mM sodium phosphate buffer (pH 7.0). A 500 μL sample was applied to a 5 mL HiTrap PhenylFF column (Pharmacia) using an Akta Purifier (Amersham), and unbound sample was washed off with 5 column volumes of 1 M ammonium sulfate and 10 mM sodium phosphate buffer (pH 7.0). The bound protein was eluted from the column using a linear salt gradient from 100% 1 M ammonium sulfate and 10 mM sodium phosphate buffer (pH 7.0) to 100% 10 mM sodium phosphate buffer (pH 7.0) at a flow rate of 2.0 mL/min, and the protein was detected at 280 nm. Subsequently, the column was washed with 5 column volumes of 10 mM sodium phosphate buffer (pH 7.0).

Intrinsic Viscosity. The flow times of filtered βlg and Gβlg solutions in 10 mM sodium phosphate buffer (pH 7.0) were measured at 25 ± 0.1 °C using an Ubbelohde capillary viscometer. The relative viscosity (η_{rel} = flow time of sample/flow time of solvent) and specific viscosity ($\eta_{sp} = \eta_{rel}^{-1}$) were calculated using the viscosity of a 10 mM sodium phosphate buffer (pH 7.0) as a solvent. Reduced viscosity ($\eta_{red} = \eta_{sp}$/sample concentration) was plotted against the sample concentration, which was varied from 0 to 10 mg/mL protein, and extrapolated to zero concentration using the Martin equation (*22*) to determine the intrinsic viscosity ([η], mL/g). The so-called Huggins constant (K') is a characteristic of a given solute−solvent system (*22*) and was calculated from the slope divided by [η] (*23*).

PRODAN Assay. A stock solution of 4×10^{-4} M PRODAN [6-propionyl-2-(*N*,*N*-dimethylamino)naphthalene] (Fluka) was prepared in methanol and protected from light. The concentration of PRODAN was determined spectrophotometrically at 360 nm, using a molar absorption coefficient of 1.8×10^4 M^{-1} cm^{-1}. A 2.5 μL PRODAN solution (or methanol: blank) was added to 1 mL of protein sample (containing 0−0.44 mM protein). Samples were incubated for 15 min in the dark, and the fluorescence intensity was measured at 25 °C using a Varian Cary Eclipse Fluorescence Spectrophotometer at an excitation wavelength of 365 nm, an emission wavelength range of 400−550 nm, and slit widths of 5 nm. The obtained fluorescence intensities were corrected for a blank containing protein and methanol. The initial slope (S_0) of the net fluorescence intensity versus PRODAN concentration (M) plot was calculated by linear regression analysis and used as a value to express the protein surface hydrophobicity.

Unfolding and Stability. *Protein Stability by Urea Titration*. Emission fluorescence spectra were recorded at a protein concentration of 2.7 μM in a phosphate buffer (10 mM, pH 7.0) using a Cary Med Eclipse (Varian) fluorometer. The samples were equilibrated overnight in 0−8 M urea at 25 °C in a 10 mM phosphate buffer (pH 7.0). The fluorescence emission was recorded between 300 and 400 nm upon excitation at 295 nm at a scan speed of 100 nm/min and excitation and emission slit widths of 5 nm. Urea titration curves were obtained by plotting the band intensity (selected at the maximum intensity of the native protein emission spectrum) for a fixed emission wavelength as a function of urea concentration.

Refolding by Stopped-Flow Fluorometry. The kinetics of refolding of a 10 mg/mL protein solution in 8 M urea and a 10 mM sodium phosphate buffer (pH 7.0) was followed using an SFM4 stopped-flow

fluorescence instrument (Biologic) using an 0.8 mm square flow cell. The unfolded proteins were diluted 10 times into a 10 mM sodium phosphate buffer (pH 7.0). The excitation and emission slit widths were 1 nm.

Kinetic Partitioning Experiments. Proteins were incubated over a range of urea concentrations (0−8 M) at pH 7.0 for 24 h at 25 °C. Then the protein/urea mixtures were diluted 10-fold in 10 mM phosphate buffer (pH 7.0). To quantify the refolding efficiency, gel permeation chromatography (GPC) was performed on the diluted samples. The quaternary structures of these samples in a 10 mM phosphate buffer (pH 7.0) containing 50 mM NaCl at 25 °C were analyzed by GPC using a 24 mL Superdex 75 column HR 10/30 (Amersham) at a flow rate of 0.4 mL/min and detection of protein in the eluent at 280 nm. The nonaggregated and aggregated fractions were collected separately. The refolded fractions of the proteins were tested for structural elements using far-UV CD and urea titrations using fluorometry and CD as described above.

Aggregation Kinetics. Various methods were employed to determine the aggregation kinetics of βlg and Gβlg.

Heat-Induced Aggregation. Heat-induced aggregates of βlg and Gβlg were formed at 7 °C below their thermal transition temperatures at pH 7.0 and a protein concentration of 0.5 mM at either a similar ionic strength of 4.2 mM or similar electrostatic repulsion of 1.21×10^{-31} C^2 m^{-1} corrected with 1 M NaCl. The electrostatic repulsion was calculated using the equation formulated by Wu et al. (*24*) and is further described under Results and Discussion. Samples were collected at various time intervals between 0 and 960 min and rapidly cooled in ice. The samples were stored at 4 °C until further analysis by GPC.

Urea-Induced Aggregation. Protein solutions were incubated at a protein concentration of 10 mg/mL and 8 M urea in 10 mM sodium phosphate buffer (pH 7.0) in autoclaved 1.5 mL Eppendorf tubes with tightly sealed lids to prevent evaporation and placed into an Eppendorf incubator at 37 °C. For each incubation time, varying from 0 to 1500 min, 10 μL aliquots were removed and rapidly cooled in liquid nitrogen, diluted 10 times in 10 mM sodium phosphate buffer (pH 7.0), and analyzed by GPC.

GPC. βLg and Gβlg solutions treated by heat or urea were diluted in 10 mM sodium phosphate buffer (pH 7.0) and 0.15 M NaCl to a final concentration of 1 mg/mL. Upon application of 100 μL of protein solution to the column (25 mL Superdex 75, Amersham), the protein was eluted from the column at a flow rate of 0.75 mL/min, and the eluted fractions were detected at 280 nm. All measurements were performed in duplicate.

RESULTS AND DISCUSSION

Our aim was to investigate previously reported effects of glycosylation on protein aggregation (*1*, *2*, *5*−*8*) in more detail. We compared the aggregation properties of glucosylated and nonglucosylated bovine βlg under a range of conditions. The glucosylation procedure employed was the Maillard reaction, which has previously been used to obtain glucosylated proteins with intact structural properties under selected incubation conditions while obtaining a significant degree of glucosylation (*13*). We first fully characterized the glycoconjugated proteins obtained in this way.

Degree of Glucosylation. The efficiency of the conjugation of D-glucose with the ϵ-amino group or the N-terminal α-amino group of βlg, which constitutes 16 potential glucosylation sites, was tested using the OPA assay and mass spectrometry. The OPA assay determines the number of nonreacted amino groups and reflects an ensemble-averaged number. This assay indicated that 14 ± 1 of 16 amino groups of the glucosylated protein were occupied by glucose residues, which corresponds to a degree of glucosylation of ~88%. As an alternative tool, mass spectrometry was used to analyze the glucosylated βlg (Gβlg) for the degree of modification, providing additional insight in the heterogeneity of the reaction products (*13*). The Gβlg spectrum showed a Gaussian distribution of masses, which is centered around 21087 Da (*13*) flanked by peaks ranging from 20229 to 21283 Da, representative of the heterogeneous distribution of Gβlg glucosylated to various degrees. Because each glucose moiety attached to a free amino group accounts for 162 Da, the average number of sugar moieties attached to the protein as found with mass spectrometry is 17, indicating a degree of glucosylation of >100%. This apparent discrepancy between the OPA assay and mass spectrometry analysis can be explained by the differences in principle of these two methods of analysis. It has been reported before (*18*) that the ϵ-amino group of arginine residues can serve as a potential glucosylation site. As each monomeric βlg molecule contains three arginine residues in the primary sequence, it is likely that this provides for additional possibilities for glucose linkage. The OPA assay specifically detects ϵ-amino acids from lysine residues as opposed to arginine residues, whereas mass spectrometry is sensitive to the total molecular mass of the formed molecule irrespective of the location of the modification.

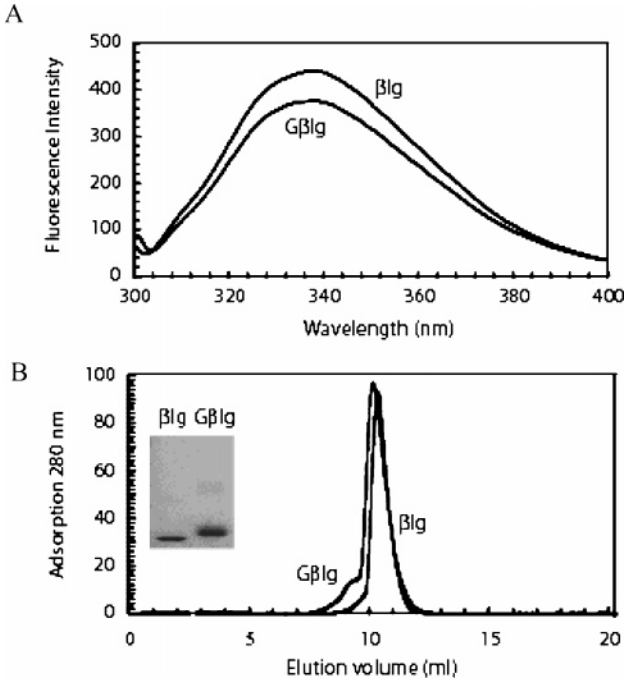

Figure 1. Structural characterization of the effect of glucosylation on βlg (**a**) intrinsic tryptophan fluorescence of βlg and Gβlg at pH 7.0 in 10 mM sodium phosphate buffer at a protein concentration of 5.5 μM (solid line, βlg and Gβlg; dashed line, Gβlg); (**b**) GPC, (inset) SDS-PAGE.

Structural Integrity. The aggregation process first involves the transition from a folded to a (partially) unfolded or extended state. Therefore, it is important to define the structural impact of the glucosylation. While modifying the primary amino groups of βlg, we therefore aimed to retain the secondary, tertiary, and quaternary structures of the nonglucosylated protein. The effect of the glucosylation on the structure of βlg was shown by a variety of techniques (**Figure 1** and *13*). The secondary structure was unaffected by the glucosylation (*13*). The far-UV CD spectra retained a similar zero-crossing (around 203 nm) upon glucosylation, and the shape of the spectrum showed extremes around 195, 210, and 218 nm, similar to βlg (*13*). Intrinsic tryptophan fluorescence studies (**Figure 1a**) showed a maximum emission intensity around 340 nm, representative of a folded conformation. Hence, the local environment of the tryptophan residues of the Gβlg was considered to be unaffected by the glycosylation procedure. Also, near-UV CD spectra indicated that the tertiary structure of the Gβlg was comparable to that of βlg (*13*). GPC (**Figure 1b**) and SDS-PAGE (**Figure 1b**, inset)

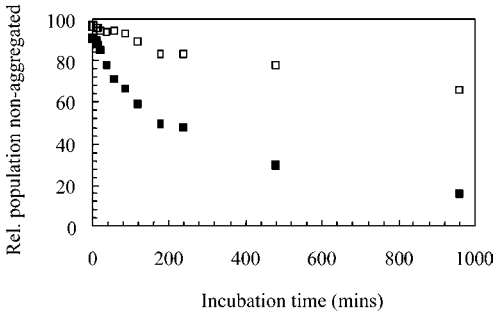

Figure 2. Glucosylation accelerates the heat-induced aggregation of βlg. The rate of disappearance of nonaggregated protein was analyzed by comparing the rates at an ionic strength of 4.3 mM [(□) βlg; (■) Gβlg] using GPC.

showed that Gβlg was a non-covalently bound dimer upon glucosylation, similar to nonglucosylated βlg (*25*−*27*). In conclusion, bovine βlg was not significantly affected at any structural level by the glucosylation procedure.

Effect of Glucosylation on the Rate of Protein Aggregation. *Heat-Induced Aggregation*. Heat-induced aggregation was used to detect variations in the aggregation rate brought about by glucosylation. Gβlg and βlg were incubated at a fixed number of 7 °C below their relative thermal transition temperatures determined by differential scanning calorimetry (see ref *13* for experimental data) to support the kinetic visualization of the aggregation process. The derived incubation temperatures were 66 °C (βlg) and 77 °C (Gβlg). It is already known that, upon unfolding, the non-covalently bound dimeric conformation of βlg (under physiological conditions) first dissociates before aggregates are formed as a result of its dissociation constant (*25*−*27*). **Figure 2** shows the loss of the nonaggregated protein using GPC as a function of the incubation time using heat-induced aggregation. The loss of the nonaggregated fraction of Gβlg is significantly faster ($k = 4.26 \times 10^{-3}$ min^{-1}) compared with the loss of the nonaggregated nonglucosylated βlg ($k = 1.74 \times 10^{-3}$ min^{-1}) (**Figure 2**).

Urea-Induced Aggregation: Variation of Urea Concentration. Temperature can significantly influence the aggregation process of βlg (*28*−*33*) as it drives partial unfolding of βlg, resulting in exposure of hydrophobic regions and thiol and disulfide groups (*28*, *29*, *31*). As the aggregation rate of βlg has been observed to be very fast, it is difficult to distinguish between the unfolding and aggregation processes using heat-induced aggregation. We therefore also investigated aggregation at ambient temperature, using urea as a denaturant. First, we determined the unfolding behavior of both Gβlg and βlg using urea titration while monitoring the shift of the tryptophan fluorescence emission maximum characteristic for unfolding (**Figure 3a**). The results show that incubation of the protein with an increased concentration of urea results in an increased fraction of unfolded protein for both Gβlg and βlg. The results also show that the midpoint for unfolding, often used to characterize protein stability, is shifted to a lower urea concentration upon glucosylation. Because we can vary the ratio of folded to unfolded protein using different urea concentrations, urea-induced aggregation following from protein unfolding can be studied.

Urea-induced aggregation was brought about by first incubating the protein solutions (10 mg/mL) at various concentrations of urea (0−8 M). Subsequent 10-fold dilution in a 10 mM sodium phosphate buffer (without urea) resulted in either aggregation or refolding (**Figure 3b**). Upon incubation of the proteins at a urea concentration below 2 M, no aggregation

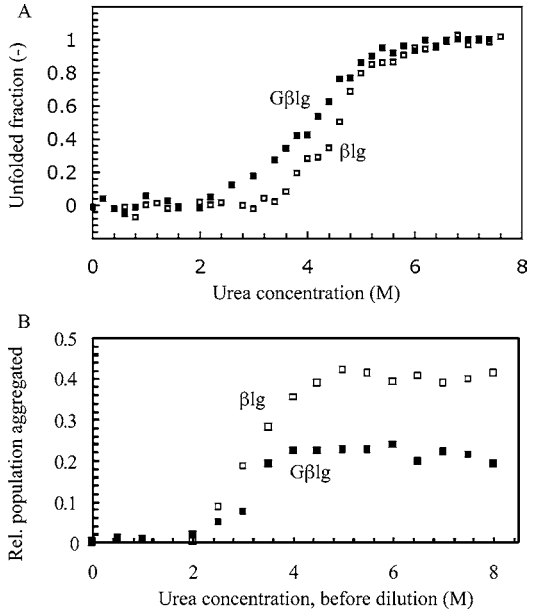

Figure 3. Glucosylation affects urea-induced unfolding and inhibits urea-induced aggregation of βlg (**a**) urea-induced unfolding of (□) βlg and (■) Gβlg using intrinsic tryptophan fluorescence (emission wavelength of 320 nm). The dashed line is to guide the eye. (**b**) Urea-induced aggregation analyzed by GPC. Samples were incubated in various urea concentrations and subsequently diluted 10 times with a buffer solution. The diluted samples were analyzed using GPC: (□) βlg; (■) Gβlg.

occurred (**Figure 3b**). The results shown in **Figure 3a** are consistent with this, suggesting that below 2 M urea for both Gβlg and βlg, no significant population of unfolded species is observed. Above a concentration of 2 M urea, a sufficient concentration of unfolded Gβlg and βlg molecules formed to drive the kinetic partitioning toward aggregation in a urea concentration dependent manner. Around 4−5 M urea, a plateau region is reached beyond which increasing urea concentration does not further change the Gβlg or βlg aggregation yield (**Figure 3b**). Also, the urea-unfolding experiment suggests no further increase in unfolded molecules beyond 4−5 M urea (**Figure 3a**). The refolded fractions of Gβlg and βlg were tested for refolded structure using far-UV CD and fluorescence. It was found that the refolded proteins did not differ structurally from the folded Gβlg and βlg (results not shown). In addition to several comparable findings between Gβlg and βlg, a number of differences in the aggregation behavior were also observed. First, the refolding yield through kinetic partitioning, under the conditions applied, is limited to approximately 57% for βlg, compared to 80% for Gβlg. In other words, glucosylation appears to limit the aggregation propensity of the protein, compared with the nonglucosylated variant. Second, even though the glucosylation process seems to destabilize the folded protein conformation (**Figure 3a**), the urea concentration at the onset of the aggregation process was not affected (**Figure 3b**).

Urea-Induced Aggregation: Kinetics. To control for any effects of changed stability on the observed differences in the aggregation rates, we investigated the aggregation process from a fully unfolded state, in 8 M urea at 25 °C (**Figure 3a**). Under these conditions βlg normally occurs as a monomeric protein as opposed to a non-covalently bound dimer at neutral pH and in the absence of urea (*26*, *27*). Subsequently, the aggregation rates of the proteins in 8 M urea were followed using GPC. In **Figure 4** the fraction of nonaggregated molecules determined by GPC is plotted against incubation time. It was found that the fractions of aggregated βlg and Gβlg increased with

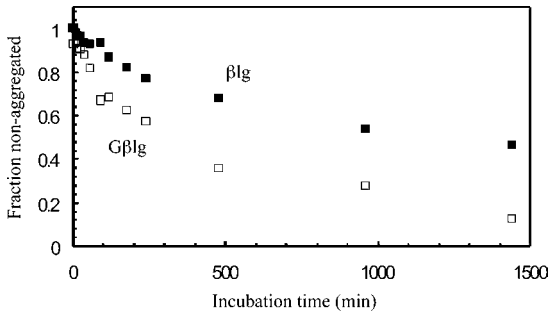

Figure 4. Glucosylation reduces urea-induced aggregation of βlg: aggregation kinetics of βlg (□) and Gβlg (■) in 8 M urea at 20 °C. The aggregation kinetics were derived from dilution from a urea-unfolded state, and the concentration of nonaggregated protein was determined using GPC.

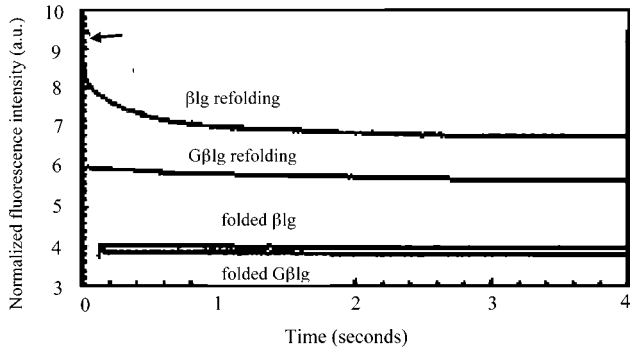

Figure 5. Glucosylation increases the refolding rate of βlg. The refolding kinetics of βlg upon glucosylation were investigated by dilution of Gβlg and βlg from 8 M urea, pH 7.0, at 25 °C. Data were recorded using a stopped-flow fluorometer λ_{ex} 295 nm and λ_{em} 320 nm. The fluorescence intensities of the unfolded proteins are indicated by an arrow.

increasing incubation time. The aggregation rates (k) were found to equal 2.81×10^{-3} and 1.86×10^{-3} min^{-1} for nonglucosylated βlg and Gβlg, respectively. The aggregation rates in **Figure 4** are clearly not identical. Glucosylation appears to inhibit the aggregation process.

How Is the Aggregation Rate of βLg Affected by Glucosylation? Interestingly, the results obtained through urea-induced aggregation are opposite to those found for heat-induced aggregation. Glucosylation accelerated heat-induced aggregation of βlg (**Figure 2**), whereas urea-induced aggregation of βlg was inhibited (**Figure 3a**). A notable difference between the two methods used to study protein aggregation is that for heat-induced aggregation, the protein molecules, once unfolded, are immediately directed toward aggregation. For urea-induced aggregation, the protein is first unfolded and no intramolecular interactions are possible. To induce the aggregation process, the urea has to be diluted. Upon dilution, the unfolded protein molecule can either refold or aggregate, depending on the activation energies for both reactions. We therefore hypothesized that the refolding rate of βlg upon glucosylation was increased, resulting in kinetic partitioning toward refolding rather than aggregation.

Refolding Efficiency. It has previously been reported that the rate of (re)folding can be increased by glycosylation (*11*, *14*). We tested if glucosylation of βlg affected the refolding rate by refolding the protein from 8 M urea and following the change of fluorescence using stopped-flow fluorescence (**Figure 5**). The fluorescence intensities of both the unfolded Gβlg and βlg started at a normalized fluorescence intensity of 9, indicated by an arrow in the figure. It is clear that for both proteins, the refolding process occurs for a large part in the dead-time of the experiment (2 ms). It is also shown that the refolding process of the glucosylated variant is already completed within this time, whereas the refolding of the nonglucosylated βlg is completed after approximately 1 s. Also, the fluorescence intensities do not recover entirely to the baseline of the completely folded proteins. This suggests an incomplete refolding process, which is consistent with the data shown in **Figure 3b**. To summarize, it was found that the attachment of glucose moieties to βlg significantly increased the refolding rate as well as the refolding efficiency tested at a protein concentration of 10 mg/mL (**Figures 4** and **5**). The results shown here suggest that the effect of glycosylation on βlg aggregation is strongly dependent on the species from which the aggregation process is started. Also, the comparison of the effect of various aggregation conditions already suggests that the kinetic parameters of refolding and unfolding potentially provide a (partial) explanation for the observed effects of glucosylation on the aggregation process. The energetic preference of glucosylated proteins to refold rather than aggregate can be explained by a variety of factors. Two factors that have been frequently related to the aggregation and/or (re)folding rate are the (exposed) hydrophobicity (*31*, *33*, *34*) and the electrostatic repulsion (*35*, *36*).

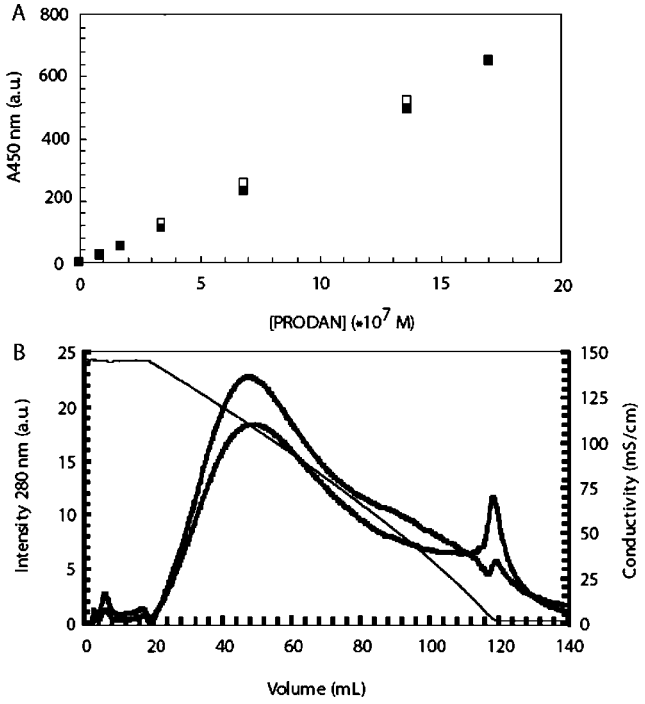

Figure 6. Glucosylation does not affect the hydrophobicity of βlg. The hydrophobicity of βlg (□) and Gβlg (■) was evaluated using (**a**) PRODAN fluorescence at pH 7.0 and (**b**) HIC.

Hydrophobicity. Glycosylation has been found to readily affect the hydrophobicity of proteins, through direct interactions of the sugar chain with the hydrophobic backbone or side residues (*37*−*39*). This potential aggregation preventative mechanism has therefore been explored in the present study in various ways. The exposed hydrophobicities of βlg and Gβlg were evaluated using three methods. First, PRODAN is an uncharged hydrophobic ligand that, upon binding to the hydrophobic regions of a protein, forms a fluorescent complex. Plotting the change in relative fluorescence intensity of βlg and Gβlg at 450 nm as a function of PRODAN concentration in the range of 0 to 1.80×10^{-6} M suggests no significant difference in exposed hydrophobicity of folded βlg and Gβlg (**Figure 6a**). It must be noted that even though the PRODAN ligand is useful for the

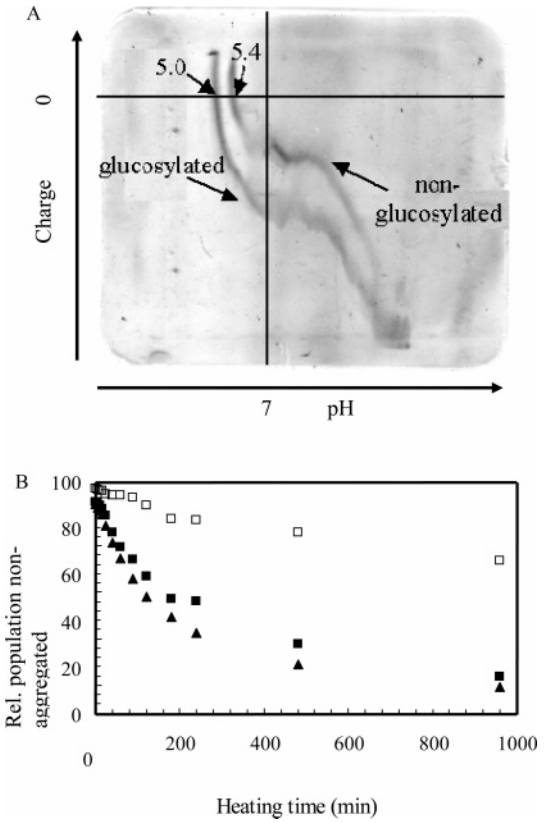

Figure 7. The effect of glucosylation on the electrostatic repulsion does not explain the differences in aggregation rates. (**a**) The electrophoretic mobilities of βlg and Gβlg were determined using electrophoretic titration curves. (**b**) The rates of disappearance of nonaggregated protein upon heat-induced aggregation were analyzed by comparing the rates at a similar ionic strength of 4.3 mM: (□) βlg; (■) Gβlg; (▲) similar electrostatic repulsion of 1.21×10^{-31} C^2 m^{-1}, Gβlg.

detection of differences in hydrophobic exposure of protein molecules, which exhibit differences in net charge (*40*), the specificity and sensitivity of the PRODAN ligand have not been unambiguously demonstrated, and therefore we confirmed the above data using HIC. The elution volume is representative of the degree of protein hydrophobicity. Nonglucosylated βlg and Gβlg both show an intensity maximum at an elution volume of 48 mL (**Figure 6b**). Further evidence for minimal contribution of exposed hydrophobicity as a factor for determination of aggregation rates upon glucosylation is provided by intrinsic viscosity experiments at pH 7.0. The Huggins constant (K') calculated from the results showed an intrinsic viscosity of 0.97 mL/mg for glucosylated βlg compared to 0.99 mL/mg for nonglucosylated βlg. These values do not indicate a significant difference, suggesting that the tendency of the folded molecules to form intermolecular interactions was not affected by glucosylation.

Electrostatics. Electrostatic repulsion significantly affects the activation barrier for long-range self-association (*35*, *36*) as well as intrinsic protein stability by, for example, stabilizing ion pairs or destabilizing repulsion (*41*). The isoelectric point of the protein upon glucosylation, as determined by IEF, was 5.0 compared with 5.4 for nonglucosylated βlg (**Figure 7a**). However, at pH 7.0, where most aggregation experiments were performed, nonglucosylated βlg has a net charge of −7 compared with −20 upon glucosylation, displaying a significant difference in net charge (calculated using Swiss-Prot application for calculating titration curves with sequence 1BEB for non-glucosylated βlg and replacing all lysines for uncharged amino acids of 1BEB for Gβlg).

Figure 4 shows the heat-induced aggregation at an ionic strength of 4.3 mM. Glucosylation significantly accelerated the aggregation rate. To investigate whether the difference in net charge found upon glucosylation through the Maillard reaction accounts for the observed differences in the aggregation rates, the ionic strength of the solution was varied. The hydrodynamic radius determined by dynamic light scattering results in values of 3.00 nm for βlg and 3.03 nm for Gβlg. Inputting these values in the equation of Wu et al. (*24*) allowed for correction of the electrostatic repulsion for the differences in net charge as calculated from theoretical titration curves. A NaCl concentration of 18 mM was required to correct the electrostatic repulsion of the Gβlg to a value (1.12×10^{-31} C^2 m^{-1}) similar to that for nonglucosylated βlg. **Figure 7b** shows the kinetics of disappearance of the nonaggregated protein peak upon heating with increasing incubation time analyzed by GPC. It is clear that correction of the electrostatic repulsion does not result in coinciding aggregation rates for βlg and Gβlg. In fact, the rate of aggregation upon correction for electrostatic repulsion ($k = 5.75 \times 10^{-3}$ min^{-1}) deviates even more from the nonglucosylated protein ($k = 1.74 \times 10^{-3}$ min^{-1}) compared with the noncorrected sample ($k = 4.27 \times 10^{-3}$ min^{-1}). Thus, even though in the past strong electrostatic repulsion has been reported as a significant inhibitor of the aggregation process, the inhibiting effect of glucosylation on the aggregation reaction cannot be explained by this mechanism.

The results reported in this paper show that glucosylation of βlg accelerates heat-induced aggregation but slows urea-induced aggregation. It was found that glucosylation can drive the kinetic partitioning toward refolding instead of aggregation. Subsequently, it was shown that the hydrophobicity was not affected by glucosylation. Correction for electrostatic repulsion differences induced by glucosylation also did not result in comparable aggregation rates. Further studies are necessary to discover the origins of the observed differences in aggregation rates upon glucosylation.

ACKNOWLEDGMENT

We acknowledge Esther Kiezebrink for conducting the Ubbelohde experiments and Jan Klok for assistance with dynamic light scattering experiments.

LITERATURE CITED

(1) Morgan, F.; Leonil, J.; Molle, D.; Bouhallab, S. Modification of bovine-lactoglobulin by glycation in a powdered state or in an aqueous solution: effect on association behavior and protein conformation *J. Agric. Food Chem.* **1999**, *47*, 83−91.

(2) Matsudomi, N.; Nakano, K.; Soma, A.; Ochi, A. Improvement of gel properties of dried egg white by modification with galactomannan through the Maillard reaction. *J. Agric. Food Chem.* **2002**, *50*, 4113−4118.

(3) Hattori, M.; Numamoto, K.; Kobayashi, K.; Takahashi, K. Functional changes in β-lactoglobulin by conjugation with cationic saccharides. *J. Agric. Food Chem.* **2000**, *48*, 2050−2056.

(4) Verma, R.; Iida, H.; Pardee, A. B. Identification of a novel stress-inducible glycoprotein in *Saccharomyces cerevisiae*. I. Preliminary characterization. *J. Biol. Chem.* **1988**, *263*, 8569−8575.

(5) Endo, Y.; Nagai, H.; Watanabe, Y.; Ochi, K.; Takagi, T. Heat-induced aggregation of recombinant erythropoietin in the intact and deglycosylated states as monitored by gel permeation chromatography combined with a low-angle laser light scattering technique. *J. Biochem. (Tokyo)* **1992**, *112*, 700−706.

(6) Heal, R.; McGivan, J. Induction of calreticulin expression in response to amino acid deprivation in Chinese hamster ovary cells. *Biochem. J.* **1998**, *329*, 389−394.
(7) Helenius, A.; Trombetta, E. S.; Hebert, D. N.; Simons, J. F. Calnexin, calreticulin and the folding of glycoproteins. *Trends Cell. Biol.* **1997**, *7*, 193−200.
(8) Land, A.; Braakman, I. Folding of the human immunodeficiency virus type 1 envelope glycoprotein in the endoplasmic reticulum. *Biochimie* **2001**, *83*, 783−790.
(9) Crabbe, M. J. Cataract as a conformational disease—the Maillard reaction, α-crystallin and chemotherapy. *Cell Mol. Biol. (Noisy-le-Grand)* **1998**, *44*, 1047−1050.
(10) Kitabatake, N.; Cuq, J. L.; Cheftel, J. C. Covalent binding of glycosyl residues to β-lactoglobulin: effects on solubility and heat stability. *J. Agric. Food. Chem.* **1985**, *33*, 125−130.
(11) Wang, C.; Eufemi, M.; Turano, C.; Giartosio, A. Influence of the carbohydrate moiety on the stability of glycoproteins. *Biochemistry* **1996**, *35*, 7299−7307.
(12) Nacka, F.; Chobert, J. M.; Burova, T.; Leonil, J.; Haertle, T. Induction of new physicochemical and functional properties by the glycosylation of whey proteins. *J. Protein Chem.* **1998**, *17*, 495−503.
(13) Broersen, K.; Voragen, A. G. J.; Hamer, R. J.; de Jongh, H. H. J. Glycoforms of β-lactoglobulin with improved thermostability and preserved structural packing. *Biotechnol. Bioeng.* **2004**, *86*, 78−87.
(14) Fenouillet, E.; Jones, I. M. The glycosylation of human immunodeficiency virus type 1 transmembrane glycoprotein (gp41) is important for the efficient intracellular transport of the envelope precursor gp160. *J. Gen. Virol.* **1995**, *76*, 1509−1514.
(15) Chiti, F.; Taddei, N.; Bucciantini, M.; White, P.; Ramponi, G.; Dobson, C. M. Mutational analysis of the propensity for amyloid formation by a globular protein. *EMBO J.* **2000**, *19*, 1441−1449.
(16) Gosal, W. S.; Clark, A. H.; Ross-Murphy, S. B. Fibrillar β-lactoglobulin gels: Part 1. Fibril formation and structure. *Biomacromolecules* **2004**, *5*, 2408−2419.
(17) Munch, G.; Schicktanz, D.; Behme, A.; Gerlach, M.; Riederer, P.; Palm, D.; Schinzel, R. Amino acid specificity of glycation and protein-AGE crosslinking reactivities determined with a dipeptide SPOT library. *Nat. Biotechnol.* **1999**, *17*, 1006−1010.
(18) Brands, S. M. J. Kinetic modelling of the Maillard reaction between proteins and sugars. 2002, Thesis, Wageningen University, Wageningen, The Netherlands, 2002.
(19) De Jongh, H. H. J.; Gröneveld, T.; de Groot, J. Mild isolation procedure discloses new protein structural properties of β-lactoglobulin. *J. Dairy Sci.* **2001**, *84*, 562−571.
(20) Church, F. C.; Swaisgood, H. E.; Porter, D. H.; Catignani, G. L. Spectrophotometric assay using *o*-phthaldialdehyde for the determination of proteolysis in milk and isolated milk proteins. *J. Dairy Sci.* **1983**, *66*, 1219−1227.
(21) Laemmli, U. K. Cleavage of structural proteins during the assembly of the head of bacteriophage T. *Nature* **1970**, *277*, 680−685.
(22) Huggins, M. L. The viscosity of dilute solutions of long-chain molecules. IV. Dependence on concentration. *J. Am. Chem. Soc.* **1942**, *64*, 2716−2718.
(23) Sakai, T. Extrapolation procedures for intrinsic viscosity and for Huggins constant *k*. *J. Polym. Sci.* **1968**, *6*, 1659−1672.
(24) Wu, J.; Bratko, D.; Prausnitz, J. M. Interaction between like-charged colloidal spheres in electrolyte solutions. *Proc. Natl. Acad. Sci. U.S.A.* **1998**, *95*, 15169−15172.
(25) Galani, D.; Apenten, R. K. Revised equilibrium thermodynamic parameters for thermal denaturation of β-lactoglobulin at pH 2.6. *Thermochim. Acta* **2000**, *363*, 137−142.
(26) Hamada, D.; Dobson, C. M. A kinetic study of β-lactoglobulin amyloid fibril formation promoted by urea. *Protein Sci.* **2002**, *11*, 2417−2426.
(27) Carrotta, R.; Arleth, L.; Pedersen, J. S.; Bauer, R. Small-angle x-ray scattering studies of metastable intermediates of β-lactoglobulin isolated after heat-induced aggregation. *Biopolymers* **2003**, *70*, 377−390.
(28) Vetri, V.; Militello, V. Thermal induced conformational changes involved in the aggregation pathways of β-lactoglobulin. *Biophys. Chem.* **2005**, *113*, 83−91.
(29) Surroca, Y.; Haverkamp, J.; Heck, A. J. R. Towards the understanding of molecular mechanisms in the early stages of heat-induced aggregation of β-lactoglobulin AB. *J. Chromatogr. A* **2002**, *970*, 275−285.
(30) Carrotta, R.; Bauer, R.; Waninge, R.; Rischel, C. Conformational characterization of oligomeric intermediates and aggregates in β-lactoglobulin heat aggregation. *Protein Sci.* **2001**, *10*, 1312−1318.
(31) Galani, D.; Apenten, R. K. Heat-induced denaturation and aggregation of β-lactoglobulin: kinetics of formation of hydrophobic and disulphide-linked aggregates. *Int. J. Food Sci. Technol.* **1999**, *34*, 467−476.
(32) Hoffman, M. A. M.; van Mil, P. J. J. M. Heat-induced aggregation of β-lactoglobulin: role of the free thiol group and disulfide bonds. *J. Agric. Food Chem.* **1997**, *45*, 2942−2948.
(33) Laligant, A.; Dumay, E.; Valencia, C. C.; Cuq, J.-L.; Cheftel, J.-C. Surface hydrophobicity and aggregation of β-lactoglobulin heated near neutral pH. *J. Agric. Food Chem.* **1991**, *39*, 2147−2155.
(34) Sava, N.; van der Plancken, I.; Claeys, W.; Hendrickx, M. The kinetics of heat-induced structural changes of β-lactoglobulin. *J. Dairy Sci.* **2005**, *88*, 1646−1653.
(35) Lopez de la Paz, M.; Goldie, K.; Zurdo, J.; Lacroix, E.; Dobson, C. M.; Hoenger, A.; Serrano, L. De novo designed peptide-based amyloid fibrils. *Proc. Natl. Acad. Sci. U.S.A.* **2002**, *99*, 16052−16057.
(36) Zurdo, J.; Guijarro, J. I.; Jiménez, J. L.; Saibil, H. R.; Dobson, C. M. Dependence on solution conditions of aggregation and amyloid formation by an SH_3 domain. *J. Mol. Biol.* **2001**, *311*, 325−340.
(37) Pieper, J.; Ott, K.-H.; Meyer, B. Stabilization of the T1 fragment of glycophorin A(N) through interactions with N- and O-linked glycans. *Nat. Struct. Biol.* **1996**, *3*, 228−232.
(38) Jentoft, N. Why are proteins O-glycosylated? *Trends Biochem. Sci.* **1990**, *15*, 291−294.
(39) Kato, A.; Nakamura, S.; Ban, M.; Azakami, H.; Yutani, K. Enthalpic destabilization of glycosylated lysozymes constructed by genetic modification. *Biochim. Biophys. Acta* **2000**, *1481*, 88−96.
(40) Haskard, C. A.; Li-Chan, E. C. Y. Hydrophobicity of bovine serum albumin and ovalbumin determined using uncharged (PRODAN) and anionic (ANS-) fluorescent probes. *J. Agric. Food Chem.* **1998**, *46*, 2671−2677.
(41) Frankenberg, N.; Welker, C.; Jaenicke, R. Does the elimination of ion pairs affect the thermal stability of cold shock protein from the hyperthermophilic bacterium *Thermotoga maritima*? *FEBS Lett.* **1999**, *454*, 299−302.

Manuscript received November 4, 2006. Revised manuscript received January 26, 2007. Accepted January 31, 2007.

JF063178Z